Journal of Catalysis **197,** 267–272 (2001)
doi:10.1006/jcat.2000.3094, available online at http://www.idealibrary.com on IDEAL®

Low-Temperature Methanol Synthesis Catalyzed over Ultrafine Palladium Particles Supported on Cerium Oxide

Yasuyuki Matsumura,[1] Wen-Jie Shen, Yuichi Ichihashi, and Mitsutaka Okumura

Osaka National Research Institute, AIST, Midorigaoka, Ikeda, Osaka 563-8577, Japan

Received April 17, 2000; revised October 11, 2000; accepted October 23, 2000; published online December 21, 2000

Ceria-supported palladium prepared by the coprecipitation method efficiently catalyzes the methanol synthesis from carbon monoxide and hydrogen at a reaction temperature as low as 170°C. The methanol yield produced with the catalyst pre-reduced at 300°C is significantly higher than with that reduced at 500°C. The catalysts contain ultrafine palladium particles that are cationic even after reduction at 500°C while a part of palladium atoms are suggested to interact directly with ceria via Pd–O–Ce bonding. The valence of the major cationic species is probably close to +1. The lower activity of the catalyst reduced at 500°C is caused from the lower surface area of palladium and less activity of the larger particles whose crystallite size is estimated to be 4 nm. © 2001 Academic Press

Key Words: **methanol synthesis; palladium; cerium oxide; ultrafine particle; EXAFS; XPS.**

INTRODUCTION

Methanol is potentially a cleaner alternative energy resource, but its cost is almost double that of crude oil at present. Thus, substantial improvement in the economics of methanol production is necessary before it can be a market competitor. Industrial methanol plants are based on the heterogeneous hydrogenation of syngas over copper–zinc catalysts, usually operated around 250°C and at a reaction pressure of more than 5 MPa for an economic rate (1). The maximum yield of methanol at 250°C is 71% in the stoichiometric reaction of carbon monoxide and hydrogen, even under the pressure of 10 MPa. To realize the conversion to methanol in one pass, which is a breakthrough in the methanol production system, the reaction must be carried out at 170°C or less due to the thermodynamic limitation; that is, a higher equilibrium yield can be attained at a lower temperature (the yield at 170°C and at 8 MPa is 92%). However, the activity of the copper–zinc catalyst, which has been improved for several decades, is not sufficient below 200°C (2). In addition, carbon dioxide must be present in the feedstock, although water is a by-product in the reaction. Palladium has been considered as an alternative metal to, and possibly more active metal than, copper; the actual activity on a weight of catalyst basis is disappointing compared with that of conventional copper catalysts (2–8). Here, we will show that a ceria-supported palladium catalyst prepared by the coprecipitation method is practically active, even at 170°C, and there is high potential for low-temperature synthesis from carbon monoxide and hydrogen. The catalyst was found to be active in methanol decomposition (9), which is a reverse reaction of the synthesis.

EXPERIMENTAL

Palladium supported on cerium oxide (15 wt% Pd/CeO_2) was prepared by coprecipitation from an aqueous mixture of $PdCl_2$ (Kishida Chemical, GR grade) and $Ce(NO_3)_3 \cdot 6H_2O$ (Kishida, 98%) by addition of an aqueous solution of 0.15 M Na_2CO_3 with vigorous stirring. The pH value of the resulting mixture was 10. The suspension was aged for 1 h under stirring and was then washed several times with distilled water until chlorine was not detected in the filtrate with a $AgNO_3$ reagent. The content of sodium was less than 0.01 wt% determined by the ICP emission spectrometry. The coprecipitate was dried in vacuum for 20 h and finally calcined in air at 500°C.

Catalytic tests were performed in a fixed-bed continuous flow reactor. A catalyst (0.5 g, 50–75 mesh), diluted with 2.0 g of quartz sand, was placed in a stainless steel tubular reactor of 9-mm i.d. (the bed length of catalyst, 40 mm). After the pre-reduction in a stream of 10 vol% hydrogen diluted with nitrogen ($3.6\ dm^3\ h^{-1}$) at 0.1 MPa for 1 h at 300 or 500°C, a mixture of carbon monoxide (33 vol%) and hydrogen (67 vol%) was introduced at a reaction temperature (170–200°C) and then the pressure was raised (total inlet flow rate, $1.8\ dm^3\ h^{-1}$ in STP). The effluent gas in which water was trapped was analyzed with two on-line gas chromatographs (Okura Riken Co. Ltd., type 802 with TCD for hydrogen, carbon monoxide, methane, and carbon dioxide and type 103 with FID for C_{1-3} hydrocarbons, methanol,

---

[1] To whom correspondence should be addressed. Present address: Research Institute of Innovative Technology for the Earth, Kizu-cho, Soraku-gun, Kyoto 619-0292, Japan. E-mail: yasuyuki@rite.or.jp. Fax: 81-774-75-2318.

0021-9517/01 $35.00

ethanol, dimethyl ether, and methyl formate). Methanol yield and selectivity were calculated on the basis of carbon numbers. The reaction was stoichiometric and the mass balance was always within the error of 2%.

The BET surface areas of the catalysts were determined from the isotherms of nitrogen physisorption.

Powder XRD (X-ray diffraction) patterns of the catalysts were recorded with a Rigaku Rotaflex 20 diffractometer using nickel-filtered Cu$K\alpha$ radiation.

X-ray photoelectron spectra (XPS) were recorded at room temperature with a Shimadzu ESCA-KM. The samples were reduced with hydrogen (0.02 MPa) for 1 h in the spectrometer. Binding energies were determined by reference to the C 1*s* binding energy of 284.6 eV.

Profiles of EXAFS (extended X-ray absorption fine structure) for the samples were taken at room temperature in transmission mode for K-edges of Pd at beam-line BL01B1 of SPring-8. The samples were reduced with hydrogen (0.02 MPa) for 1 h in a vacuum system and sealed with polyethylene films under a nitrogen atmosphere. The Fourier transformation was performed on k^3-weighted EXAFS oscillations in the range of 3–15 Å^{-1}. Normalization of the EXAFS was done by dividing the absorption intensity by the height of the absorption edge. A cubic spline background subtraction was carried out. Inverse Fourier transform was obtained within the windows 1.9–2.8 Å for Pd–Pd or 1.1–1.9 Å for Pd–O in *r* space. The Pd–Pd and Pd–O references were derived from the EXAFS of Pd foil and PdO (Kishida), respectively. The analysis was performed with a program of "REX" supplied by Rigaku.

RESULTS

Methanol Synthesis over 15 wt% Pd/CeO$_2$

Methanol was selectively synthesized at 200°C from carbon monoxide and hydrogen at 2.0 MPa over ceria-supported palladium (15 wt% Pd/CeO$_2$) pre-reduced at 300°C for 1 h with hydrogen (Fig. 1). The catalytic activity increased in the initial stage of reaction, decreased slightly, and then stabilized after 15 h on-stream. The catalyst yielded 18.3% of methanol after 24 h on-stream with a selectivity of 97.6% The by-product was mainly methane with slight amounts of ethane and dimethyl ether. With the palladium catalyst pre-reduced at 500°C, the methanol yield was only 3.6% after 24 h on-stream (selectivity, 97.1%). At a reaction temperature of 170°C 15 wt% Pd/CeO$_2$ reduced at 300°C was still active (see Fig. 1, solid circles). The activity was low at the initial stage, but increased significantly up to 15 h on-stream at 3.0 MPa. The pre-reduction of the catalyst at 300°C for 3 h did not increase the activity at the initial stage, showing that the phenomenon is not due to an insufficient reduction. Methanol yield at 170°C was linearly increased with an increase in the reaction pressure (Fig. 2). The activity was measured after 20 h on-stream. The selectivity to methane at 170°C was significantly smaller than that at 200°C, i.e., 0.7% at 1.0 MPa and 0.5% at 2.0 and 3.0 MPa. At 3.0 MPa ethanol was also by-produced with the selectivity of 1.4%.

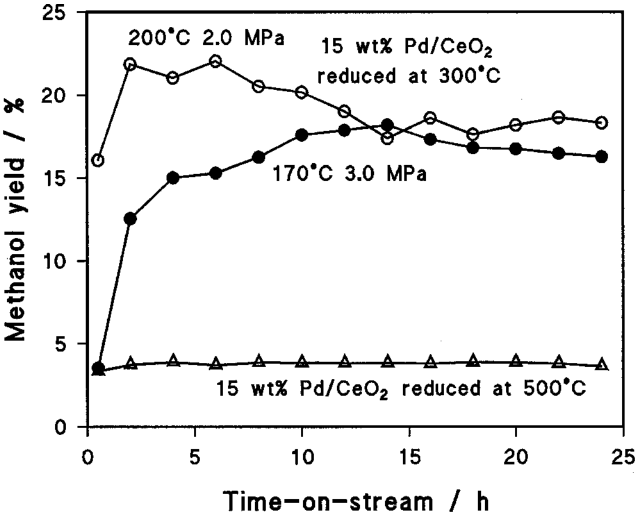

FIG. 1. Catalytic activity of pre-reduced 15 wt% Pd/CeO$_2$ for methanol synthesis at low reaction temperatures.

Structural Analyses of 15 wt% Pd/CeO$_2$

Although the catalyst contained 15 wt% of palladium, the major XRD (X-ray diffraction) peak for metallic palladium at 39.9° in 2θ (10) was very weak and broad in the pattern for the sample reduced at 300°C (Fig. 3). The peaks attributable to cerium oxide (10) were recorded at $2\theta = 28.6°$, 33.1°, and 47.5°. Reduction at 500°C developed a clear peak for palladium at 40.1°.

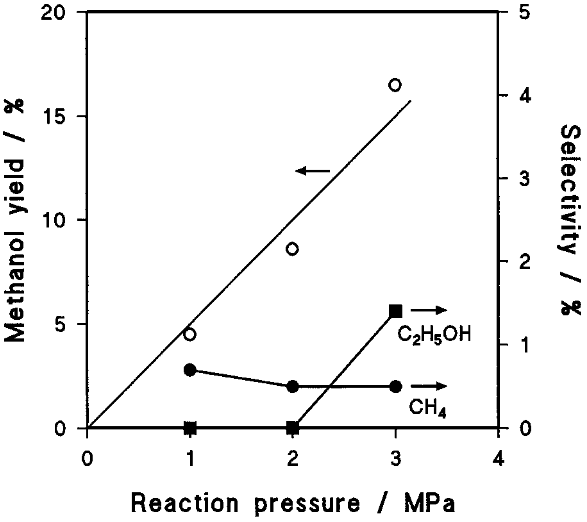

FIG. 2. Pressure dependence of methanol synthesis at 170°C over 15 wt% Pd/CeO$_2$ reduced with hydrogen at 300°C.

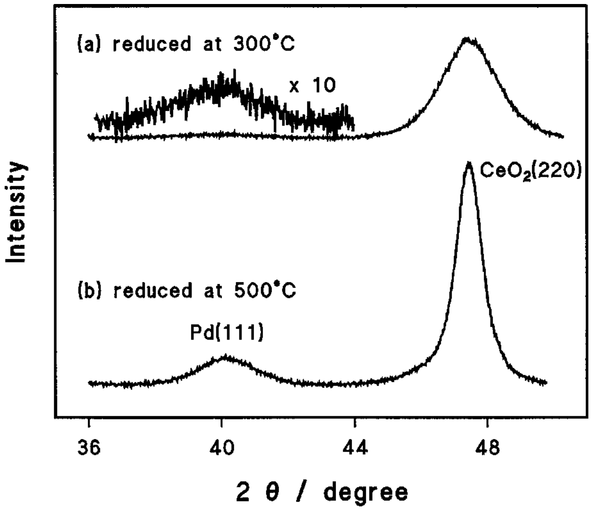

FIG. 3. XRD patterns of 15 wt% Pd/CeO$_2$ reduced with hydrogen at (a) 300°C and (b) 500°C.

The BET surface areas were 120 and 35 m^2 g^{-1} for the samples reduced at 300 and 500°C, respectively.

The Pd K-edge X-ray absorption near-edge structure (XANES) of 15 wt% Pd/CeO$_2$ reduced at 500°C was similar to that of palladium foil, but the XANES for the sample reduced at 300°C was significantly different from these profiles and rather similar to the profile of palladium oxide (Fig. 4). The Fourier transform of the Pd K-edge EXAFS for the sample reduced at 300°C showed a major peak at 2.4 Å with a minor peak at 1.6 Å (Fig. 5). The major peak is attributed to Pd–Pd bonding of the metal (11) and the position of the minor peak was very similar to that of Pd–O in the profile of palladium oxide. The coordination numbers and distances determined by curve fitting are described in Table 1. After reduction at 500°C, the peak attributed to Pd–Pd bonding was considerably intensified (see Fig. 5), and the coordination number of Pd–Pd was significantly larger than that for the sample reduced at 300°C.

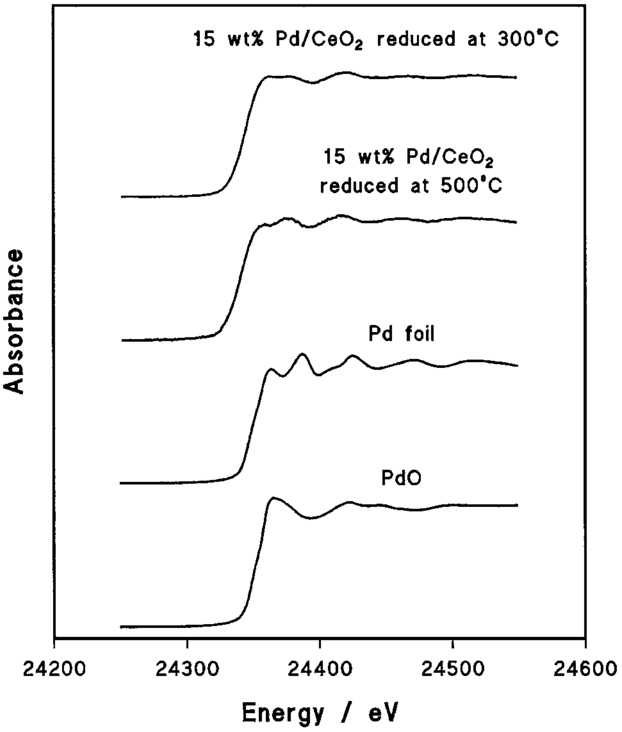

FIG. 4. Pd K-edge XANES spectra of 15 wt% Pd/CeO$_2$ reduced with hydrogen.

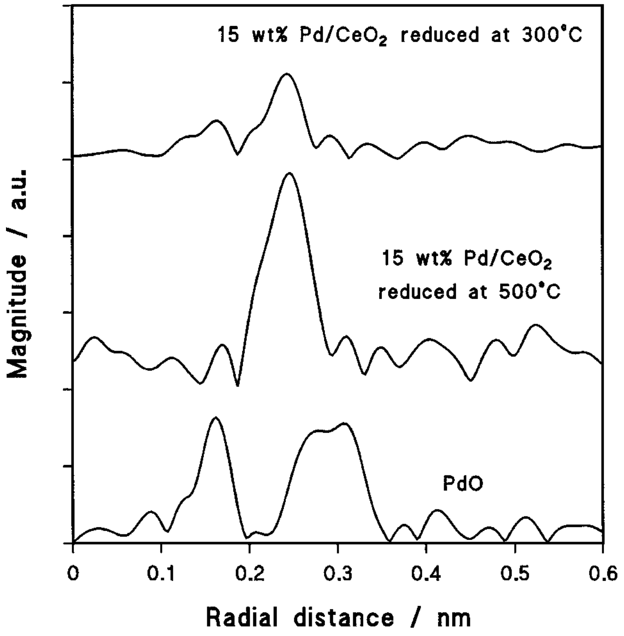

FIG. 5. Fourier-filtered Pd K-edge pseudoradial distribution functions of 15 wt% Pd/CeO$_2$ reduced with hydrogen.

Surface Properties of 15 wt% Pd/CeO$_2$

Surface analyses by XPS (X-ray photoelectron spectroscopy) were performed with the palladium sample reduced *in situ*. In the Pd 3$d_{5/2}$ region, there were peaks at 335.9 and 338.2 eV in the XPS of the 300°C sample (Fig. 6).

TABLE 1

EXAFS Parameters for 15 wt% Pd/CeO$_2$

Sample	Bonding	Interatomic distance, R (nm)	Coordination number, N	Debye–Waller factor, σ (nm)
Pd foil	Pd–Pd	0.275	12.0	0.0060
Pd/CeO$_2$ (300°C)[a]	Pd–Pd	0.270	3.4	0.0078
Pd/CeO$_2$ (500°C)[b]	Pd–Pd	0.273	8.0	0.0070
PdO	Pd–O	0.202	4.0	0.0060
Pd/CeO$_2$ (300°C)	Pd–O	0.200	2.9	0.0111

[a] 15 wt% Pd/CeO$_2$ reduced with hydrogen at 300°C for 1 h.
[b] 15 wt% Pd/CeO$_2$ reduced with hydrogen at 500°C for 1 h.

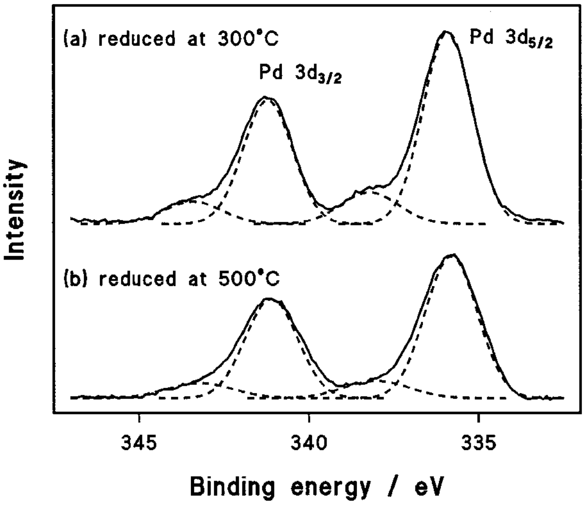

FIG. 6. XPS of Pd 3*d* region for 15 wt% Pd/CeO_2 reduced with hydrogen at (a) 300°C and (b) 500°C. Broken curves are the result of peak deconvolution using Gauss functions.

In the spectrum of the sample reduced at 500°C the major peak was at 335.8 eV while a minor peak at 338.0 eV was still visible.

The major peak of Ce $3d_{5/2}$ was at 882.6 eV for both the samples reduced at 300 and 500°C (Fig. 7). Since the peak at 917 eV (u''') is attributed to the transitions to the final state $4f^0$ from the initial state $4f^0$ (12) and the $4f^0$ configuration is lacking in the formal Ce^{3+} state, there is no peak of u''' in the spectrum for Ce^{3+} species (13). Hence, the percentage of the peak area for u''' in the whole Ce 3*d* region is a parameter of the relative amount of Ce^{4+} in the sample (13). The values calculated for the samples reduced at 300 and 500°C were almost the same and were 6.5 and 6.4%, respectively. The value of %u''' for oxidized CeO_2 was reported to be 13.7% (13). The peaks at ca. 885 eV (v') associated with Ce^{3+} states were also present (14).

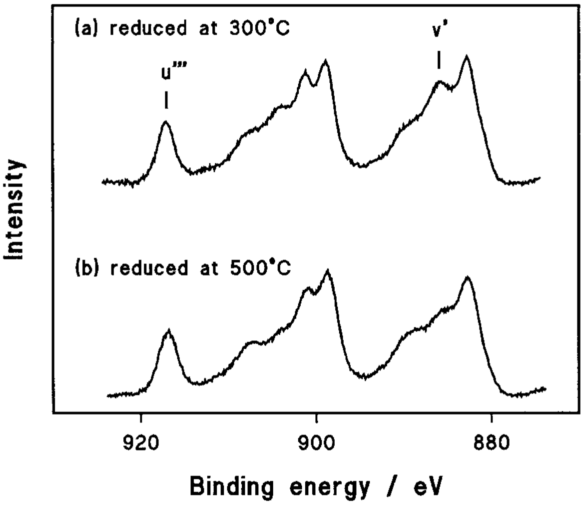

FIG. 7. XPS of Ce 3*d* region for 15 wt% Pd/CeO_2 reduced with hydrogen at (a) 300°C and (b) 500°C.

The same binding energy of 529.8 eV was recorded as O 1*s* for these samples. The value is very close to that for the oxygen in CeO_2 (15), indicating the charging effect is well cancelled. The surface molar ratio of Pd/Ce/O for the sample reduced at 300°C was estimated as 4/32/64 from the XPS peak areas using the atomic sensitivity factors of Pd 3*d* (4.6), Ce 3*d* (10), and O 1*s* (0.66), and it is very similar to that for the sample reduced at 500°C, i.e., 4/33/63 (16).

DISCUSSION

Paticle Size of Palladium in 15 wt% Pd/CeO_2

The approximate mean crystallite size of palladium in the catalyst reduced at 300°C can be calculated as 3 nm from the line broadening of the XRD peak at 39.9° using Sherrer's equation (17). However, there may be a substantial number of palladium particles smaller than 3 nm, which are invisible to X-rays because the peak intensity is very weak although the sample contains 15 wt% of palladium. The mean crystallite size of palladium in the sample reduced at 500°C is estimated as 4 nm from the XRD peak at 40.1°. After the reduction at 500°C the peak attributed to Pd–Pd in the Fourier transform of the EXAFS is significantly intensified in comparison with that after reduction at 300°C (see Fig. 5), showing an increase in the size of palladium particles by treatment at 500°C (18). The smaller Debye–Waller factor of Pd–Pd for the sample reduced at 500°C suggests the higher crystallinity and it is consistent with the larger particle size (see Table 1). Prediction of particle size for metallic species from the EXAFS data has gained widespread use. The standard procedure was proposed by Greegor and Lytle (18, 19) and the particle sizes of palladium in the samples reduced at 300 and 500°C can be estimated as 0.5 and 1.6 nm, respectively. Clausen *et al.* criticized the procedure on the basis of molecular dynamics simulations and they showed that the particle size determined by the standard method is underestimated (20). However, in conjunction with the information from the XRD measurement, it is believed that the palladium particles in the catalyst reduced at 300°C are ultrafine and significantly smaller than those in the sample reduced at 500°C. Since the magnitude of the peak of Pd–O for the sample reduced at 300°C in Fig. 4 is considerably small compared with the peak for Pd–Pd, the presence of Pd–O does not largely affect the estimation of the palladium particle size. The crystallite sizes of cerium oxide in the samples reduced at 300 and 500°C are estimated as 4 and 9 nm, respectively, from the width of the XRD peak at 47.5°. Assuming that the particles of cerium oxide are all isolated and spherical, the surface area can be calculated as 146 and 70 m^2 g-cat^{-1} for the samples reduced at 300 and 500°C, respectively. Since these values correspond roughly to the BET surface area of 120 and 35 $m^2 g^{-1}$, ceria particles are not highly aggregated.

Oxidation State of Palladium in 15 wt% Pd/CeO$_2$

The binding energies of 335.9 and 335.8 eV for Pd $3d_{5/2}$ in the XPS of the samples reduced at 300 and 500°C, respectively, are significantly higher than that of palladium metal at 335.0 eV (16), showing that the palladium species in the samples are cationic. The binding energy of Pd $3d_{5/2}$ for PdO is 336.3 eV (16) and Kili *et al.* reported that the peak at 336.8 ± 1 eV is attributed to PdO in Pd/γ-Al_2O_3 modified with cerium or lanthanum oxide (21). Since the valence of palladium generally relates to the binding energy (16), the valence of the major palladium species in the samples is probably close to $+1$. The peak attributed to Pd–Pd bonding is dominant in the Fourier transform of the EXAFS for the sample reduced at 500°C, indicating that the palladium is mostly reduced to the metal. Thus, the higher binding energy of Pd $3d_{5/2}$ is not arisen from palladium oxide, implying strong interaction between the palladium particles and cerium oxide. The minor peak of Pd $3d_{5/2}$ at 338.2 eV can be attributed to the palladium atom connecting to the oxygen atom. However, the binding energy is significantly higher than that of PdO (16) and we may infer that the Pd–O bonding does not belong to Pd–O–Pd but rather to Pd–O–Ce (15, 22). The presence of Pd–O bonding is also shown in the EXAFS of the sample reduced at 300°C. The large Debye–Waller factor for the Pd–O indicates that the bonding is highly disordered, and the presence of Pd–O–Ce may cause it. Although the presence of the Pd–O bonding is insignificant in the Fourier transform of the EXAFS for the sample reduced at 500°C, the peak at 338.2 eV can be deconvoluted from the XPS for the sample, suggesting the presence of Pd–O–Ce, which may cause the formation of the palladium species whose valence is close to $+1$. The surface of the ceria support is considerably reduced. It would affect the formation of the bonding of Pd–O–Ce, but the detailed study is necessary to clarify the interaction between the palladium particles and the support.

Catalytic Activity of Palladium

Ponec has pointed out the importance of Pd^+ for promotion of methanol synthesis (23–25). In the palladium catalyst prepared by coprecipitation the cationic species can be present under reductive conditions by virtue of strong interaction between the ultrafine palladium particles and the ceria support. The space time yield (STY) of methanol is generally employed for comparison of methanol synthesis catalysts while it depends on the reaction pressure and the value of F/W, especially when the conversion is close to the equilibrium. That produced with the coprecipitated catalyst reduced at 300°C is 8.7 mmol $h^{-1} g^{-1}$ at 170°C and at 3.0 MPa. The value is comparable with those of commercial copper catalysts for methanol synthesis at 230°C while we assumed that the STY is parallel to the reaction pressure to estimate the value at 3.0 MPa and the density of the catalysts is 1.8 kg dm^{-3} (2, 26). The binding energy of Pd $3d_{5/2}$ for ceria-supported palladium catalysts prepared by the conventional impregnation method were reported to be close to that for metallic palladium (15, 22, 27), and the activity of the catalysts was not outstanding (6, 7, 15). The STY was reported to be 0.6 mmol $h^{-1} g^{-1}$ over impregnated 3 wt% Pd/CeO_2 at 250°C and at 2 MPa (15) and that with impregnated 1.6 wt% Pd/CeO_2 was 0.07 mmol $h^{-1} g^{-1}$ at 250°C and at 1.5 MPa (6). Since the methanol yield relates to the reaction pressure as shown in Fig. 2, we can expect that the reaction over the coprecipitated catalyst at a high pressure close to 10 MPa with a lower space velocity will yield sufficient methanol conversion, which enables one-pass operation, while the test was not carried out due to the pressure limitation of our reactor.

The surface area of palladium for the samples reduced at 300 and 500°C can be estimated as 7 and 2 $m^2 g^{-1}$, respectively, from the BET surface area and the surface molar ratios using the atomic cross sections of Pd (0.060 nm^2), Ce^{4+}(0.022 nm^2), and O^{2-} (0.023 nm^2) (9). The tentative turnover frequency (TOF) for the Pd calculated from the methanol yield at 170°C and at 3.0 MPa is 46 h^{-1}. Since the TOF for Cu in the supported catalysts at 240 or 250°C and at 5.0 MPa calculated from the data in Refs. (1, 28) is around 30 h^{-1} (the site density of 19.2 nm^{-2} was calculated from the density of the metal), palladium can produce activity similar to that of copper at a significantly lower temperature. The TOF of Pd in impregnated 1.6 wt% Pd/CeO_2 was reported to be only 9 h^{-1} in the reaction at 250°C and at 1.5 MPa (6), indicating that the cationic palladium is advantageous to the metallic species in the synthesis. The TOFs for the catalysts reduced at 300 and 500°C in the reaction at 200°C and at 2.0 MPa are calculated to be 38 and 26 h^{-1}, respectively, suggesting that the smaller palladium particles are rather active in the reaction. Assuming that the palladium particles are spherical with 3 nm in diameter, the surface area of 15 wt% of palladium should be 25 $m^2 g^{-1}$ instead of 7 $m^2 g^{-1}$. This simple calculation shows that the palladium particles in the coprecipitated catalyst are not effectively exposed on the surface and the higher catalytic activity will be produced with a smaller amount of palladium by improvement in the preparation technique.

The mechanism for methanol synthesis over palladium has not been clear yet, but it is believed that carbon monoxide is directly hydrogenated while methyl formate is the intermediate in the case of liquid-phase methanol synthesis at low temperatures in the presence of base catalysts (2, 29). Naito *et al.* proposed that reduction of cerium oxide causes the formation of methane over ceria-supported palladium (30). Since the reduction of cerium oxide will proceed at a higher reaction temperature, the by-production of methane may be preferable at a higher reaction temperature. In actuality, the selectivity to methane at 170°C is considerably lower than that at 200°C, showing that the operation at 170°C will lessen the formation of methane.

CONCLUSIONS

Ultrafine palladium particles less than 3 nm can be prepared on a ceria support by the copreciptation method. The palladium species on the surface is cationic and the valence is probably close to +1, even after reduction with hydrogen at 500°C by which pretreatment the particle size is considerably larger than that reduced at 300°C. Structural analysis by EXAFS of the sample shows the presence of Pd–O bonding, which is suggested to belong to Pd–O–Ce. Methanol can be selectively synthesized from carbon monoxide and hydrogen at a reaction temperature as low as 170°C over the ultrafine palladium catalyst. The turnover frequency of the catalyst is significantly higher than that of the copper–zinc catalyst. Methanol yield produced with the palladium catalyst pre-reduced at 300°C is significantly higher than that with the catalyst reduced at 500°C. Lower activity of the catalyst reduced at 500°C is caused from the lower surface area of palladium and the lesser activity of the larger palladium particles in the solid.

ACKNOWLEDGMENTS

The synchroton radiation experiment was performed with the approval of the Japan Synchrotron Radiation Research Institute (Proposal 1998A0050-NX-NP). W.S. acknowledges the fellowship of the New Energy and Industrial Technology Development Organization of Japan.

REFERENCES

1. Chinchen, G. C., Mansfield, K., and Spencer, M. S., *CHEMTECH* 692 (1990).
2. Chinchen, G. C., Denny, P. J., Jennings, J. R., Spencer, M. S., and Waugh, K. C., *Appl. Catal.* **36**, 1 (1988).
3. Poutsma, M. L., Elek, L. F., Risch, P. A., and Rabo, J. A., *J. Catal.* **52**, 157 (1978).
4. Lunsford, J. H., *in* “Catalysis of Organic Reactions” (R. L. Augustine, Ed.), Vol. 22, p. 95. Dekker, New York, 1985.
5. Cavalcanti, A. P., Stakheev, A. Y., and Sachtler, W. M. H., *J. Catal.* **134**, 226 (1992).
6. Sudhakar, C., and Vannice, M. A., *J. Catal.* **95**, 227 (1985).
7. Fan, L., and Fujimoto, K., *J. Catal.* **150**, 217 (1994).
8. Naito, S., Aida, S., Tsunematsu, T., and Miyao, T., *Chem. Lett.* **1998**, 941.
9. Usami, Y., Kagawa, K., Kawazoe, M., Matsumura, Y., Sakurai, H., and Haruta, M., *Appl. Catal. A* **171**, 123 (1998).
10. JCPDS files, 5-0681 and 34-0394.
11. Kim, K. S., Gossmann, A. F., and Winograd, N., *Anal. Chem.* **46**, 197 (1974).
12. Fujimori, A., *Phys. Rev. B* **28**, 2281 (1983).
13. Shyu, J. Z., Weber, W. H., and Gandhi, H. S., *J. Phys. Chem.* **92**, 4964 (1988).
14. Laachir, A., Perrichon, V., Badri, A., Lamotte, J., Catherine, E., Lavalley, J. C., El Fallah, J., Hilaire, L., Le Normand, F., Quéméré, E., Sauvion, G. N., and Touret, O., *J. Chem. Soc. Faraday Trans.* **87**, 1601 (1991).
15. Shen, W.-J., Ichihashi, Y., and Matsumura, Y., *Catal. Lett.* **64**, 23 (2000).
16. “Practical Surface Analysis (Second Edition) Vol. 1: Auger and X-ray Photoelectron Spectroscopy” (D. Briggs and M. P. Seah, Eds.), Wiley, New York, 1990.
17. Klug, H. P., and Alexander, L. E., “X-ray Diffraction Procedures.” Wiley, New York, 1954.
18. Greeegor, R. B., and Lytle, F. W., *J. Catal.* **63**, 476 (1980).
19. Matsumoto, H., and Tanabe, S., *J. Phys. Chem.* **99**, 6951 (1995).
20. Clausen, B. S., Gråbæk, L., Topsøe, H., Hansen, L. B., Stoltze, P., Nørskov, J. K., and Nielsen, O. H., *J. Catal.* **141**, 368 (1993).
21. Kili, K., Hilaire, L., and Le Normand, F., *Phys. Chem. Chem. Phys.* **1**, 1623 (1999).
22. Shen, W.-J., and Matsumura, Y., *Phys. Chem. Chem. Phys.* **2**, 1519 (2000).
23. Driessen, J. M., Poels, E. K., Hindermann, J. P., and Ponec, V., *J. Catal.* **82**, 26 (1983).
24. Ponec, V., *Catal. Today* **12**, 227 (1992).
25. Ponec, V., *Surf. Sci.* **272**, 111 (1992).
26. Herman, R. G., Klier, K., Simmons, G. W., Finn, B. P., Bulko, J. B., and Kobylinski, T. P., *J. Catal.* **56**, 407 (1979).
27. Fan, L., and Fujimoto, K., *J. Catal.* **172**, 238 (1997).
28. Pan, W. X., Cao, R., Roberts, D. L., and Griffin, G. L., *J. Catal.* **114**, 440 (1988).
29. Marchionna, M., Basini, L., Aragno, A., Lami, M., and Ancillotti, F., *J. Mol. Catal.* **75**, 142 (1992).
30. Naito, S., Aida, S., and Miyao, T., *Stud. Surf. Sci. Catal.* **130**, 701 (2000).